

# Experimental investigation of the entropy noise mechanism in aero-engines

**F. Bake<sup>\*</sup>, N. Kings<sup>†</sup>, A. Fischer<sup>‡</sup> and I. Röhle<sup>§</sup>**

*German Aerospace Center (DLR) Institute of Propulsion Technology*

*Department of Engine Acoustics Müller-Breslau-Straße 8, 10623 Berlin, Germany*

It is assumed by theory, that entropy noise emitted by combustion systems increases rapidly with rising Mach number in the nozzle downstream of the combustion chamber. Model experiments have been carried out to verify the existence of this sound generating mechanism. A dedicated test facility was built, in which entropy waves are generated in a controlled way by unsteady electrical heating of fine platinum wires immersed in the flow. Further experiments have been carried out in a model combustor test rig where a broadband noise phenomenon, presumably related to indirect noise generation mechanisms, was found.

## 1. INTRODUCTION

The total noise emitted by a gas turbine combustion system can be divided into direct noise caused by the unsteady combustion itself and indirect combustion noise also called entropy noise. Only the direct combustion noise is related to the combustion process and results from local fluctuations in heat release processes and from temporal changes in momentum rates. Indirect combustion noise also called entropy noise originates from convecting gas temperature nonuniformities in an accelerated flow. In aero-engines the combustor flow is strongly accelerated into the first turbine stage at the combustor outlet. Since the nozzle guide vanes (NGV) of the first turbine stage are choked under almost every relevant operation condition, hot spots passing through the nozzle are connected with mass flow variations (monopole sound source) and also with momentum flux variations (dipole sound source). For critical conditions in the minimum cross sectional area the flow velocity is proportional to the square root of the temperature.

Therefore, a temperature fluctuation causes a velocity fluctuation and generates indirect noise. Entropy noise receives increased interest by the aero-engine industry because it may have a major contribution to the total noise emission of combustion systems. Indirect noise or entropy noise was predicted theoretically in the 70th by Strahle (16), Marble and Candel (10), and Cumpsty (3). A generalized acoustic energy equation including terms of direct and indirect noise has been given by Dowling (5). Numerical simulations of indirect noise have been shown by Schemel (15). Recently the existence of entropy noise was demonstrated experimentally by Bake et al. (1) for a rotational-free low disturbance inlet flow. In a review work concerning different combustion noise sources Strahle (19) concluded that the impact and importance of entropy noise is still controversial in the literature which is mainly caused by the lack of comprehensive experimental investigations in this area. This deficiency of experimental entropy noise research holds on even up to now.

\*friedrich.bake@dlr.de

†nancy.kings@dlr.de

‡andre.fischer@dlr.de

§ingo.roehle@dlr.de

Main challenge for investigating experimentally entropy noise is the separation of direct and indirect combustion noise. Muthukrishnan and Strahle (18; 13) separated direct noise sources and entropy noise in a combustor rig via coherence analysis. An experimental approach with the generation of entropy waves by electrical heaters similar to the test rig presented here was done by Bohn (2) and Zukoski (20) in the seventies. However, the used experimental setup generated only a very low temperature modulation ( $\approx 1$  K) with little parameter variations and the data acquisition and processing system did not allow a high-resolution quantitative signal analysis in the time domain. Therefore, the generation mechanisms and parameter dependencies of entropy noise are still not completely explained so far. Hence, this work within the framework of a DFG research unit on combustion noise (<http://www.combustion-noise.de>) presents an investigation of entropy noise phenomena in a reference test rig called Entropy Wave Generator (EWG) and in a downscaled aero-engine combustor.

With noise reduction improvements achieved in other aero-engine components by realising e.g. low noise fan design or jet noise reduction by high bypass ratios, the noise concern in aero-engine developments also includes the combustion noise issue. Especially at helicopter engines, which do almost emit no jet noise, entropy noise seems to be of high importance. Up to now there is still uncertainty about the contribution of indirect combustion noise to the total noise emission as well as the dominating frequency range.

## **2. EXPERIMENTAL FACILITIES**

The experiments have been conducted at two different test rigs - at the Entropy Wave Generator and the Model

Combustor Rig. In the non-reactive reference test rig, called Entropy Wave Generator (EWG) the sound emission of artificially induced entropy waves in an accelerated tube flow can be investigated. The idea of this set-up is to test and optimise detection methods for entropy noise and to study the parameter dependencies of the entropy noise generation mechanism. In addition the EWG allows with its well-defined boundary conditions the validation of numerical simulations and the comparison with theoretical considerations. The received knowledge at the EWG can be transmitted and applied to the complex combustor test rig. In this Combustor Test Rig the noise emitted by accelerated entropy perturbations in case of a reactive combustor flow can be analysed.

### **2.1. THE ENTROPY WAVE GENERATOR SET-UP**

The Entropy Wave Generator is basically an accelerated tube flow extended by the possibility of inducing entropy waves via a heating module. A sketch of the design is shown in Fig. 1. The flow supplied by compressed air is calmed in a settling chamber with an integrated honeycomb flow straightener before it enters the tube section of an inside diameter of 30 mm through a bell-mouth intake. The following heating module is 48 mm in length and consists of six ring sections with ten platinum wires stretched across each section resulting in a total wire length of 1.2 m. The wire itself measures 25 mm in diameter. In the current set-up the electrical power supplying the heating wires is up to 200 W. The tube section after the heating module is variable in length so that distances between heating module and nozzle throat of 50, 100 or 200 mm can be tested. In the two longer tube sections a bare wire thermocouple with a diameter of 25 mm can be installed in order to obtain information about the convecting entropy waves by

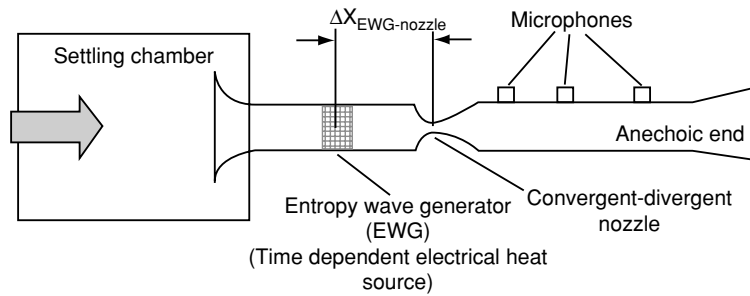


Figure 1. Sketch of the entropy wave generator; Tube section  $\Delta X_{EWG-nozzle}$  is variable, corresponding to different propagation lengths of entropy waves.

measuring the temperature fluctuations. This fast thermocouple is located in both tube sections 34 mm downstream of the heating module. The flow entering subsequently the convergent-divergent nozzle is accelerated at first in the convergent part and then decelerated in the subsonic divergent diffuser part of the nozzle. The maximum Mach number in the nozzle throat amounts to  $Ma = 1$  at a mass flux of about 11 g/s and a nozzle diameter of 7.5 mm. The maximum mass flux in the test rig is limited by the air supply to 18 g/s. The following 1020 mm long tube section measures 40 mm in diameter and is equipped with wall-mounted microphones at different axial positions for acoustic measurements. The flow leaves the test rig through an anechoic termination to minimize acoustic reflections into the measurement section.

## 2.2. THE COMBUSTOR TEST RIG SET-UP

The combustor used for experimental investigation is designed to replicate a fuel-air mixing characteristic of full-scale gas turbine combustor while still permitting analysis by experimental means. The power consumption can be varied from 5 kW to 20 kW at different air ratios from  $\lambda = 0.8$  to  $\lambda = 1.8$ . These air ratios can be converted into equivalence ratios from  $\phi = 1.25$  to  $\phi = 0.55$  applying the definition  $\phi = 1/\lambda$ . The axially symmetric test rig consists

of three sections: the combustion chamber, the convergent-divergent outlet nozzle, and the exhaust duct. A swirl generating dual air-flow nozzle is used to drive the combustion zone with non-preheated air. Methane gas is injected as fuel through an annular slot between the air streams. The combustion chamber itself is made of a fused quartz glass or steel cylinder with 100 mm inner diameter. A convergent-divergent nozzle that simulates the acceleration through the first turbine stage terminates the combustion chamber (see Fig. 2) The outlet nozzle is attached to an exhaust duct with the same diameter as the combustion chamber. In order to reduce the impedance jump at the exhaust outlet, an end diffuser perforated with holes of 2 mm diameter and with increasing perforation density toward the exit is installed.

Sound pressure measurements in combustion environments make high demands on the acoustic equipment. High temperatures, up to 2000 K, and high corrosive exhaust gases preclude the usage of classical microphone set-ups. To prevent sensor destruction a probe microphone configuration is used. Due to the spatial separation of the measurement location at the combustion chamber wall or exhaust duct and the microphone itself, common 1/4 inch microphones can be used. A steel tube of 2 mm inner diameter realizes the connection between the exhaust duct wall and the

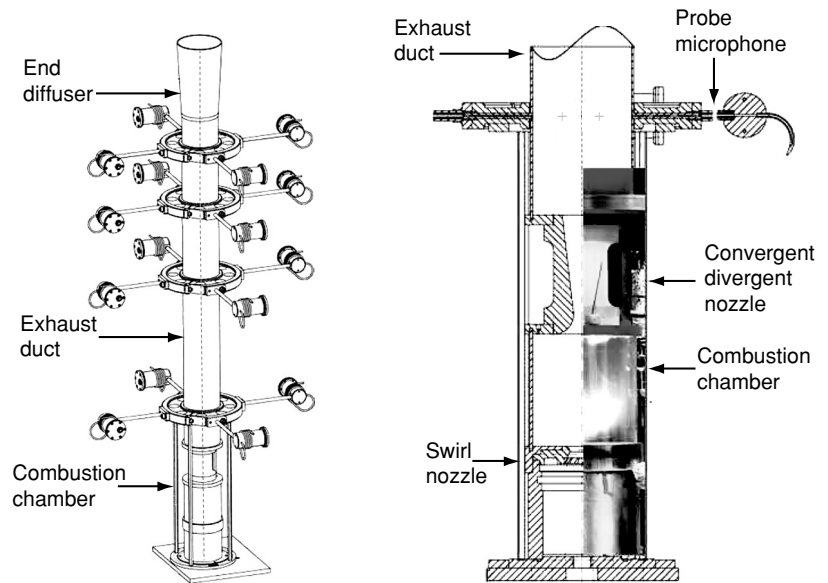


Figure 2. *Isometric view (left) and sketch (right) including a picture of the combustor test facility.*

microphone. For impedance matching and for minimizing standing wave effects the probe tube is extended according to the principle of a semi-infinite acoustic duct. The microphone itself is perpendicular and wall-mounted inside the cylindrical chamber or exhaust duct. From the rear end, the probe tube is purged with cooling gas with a well-controlled small flow rate. The air purging prevents damage of the microphone diaphragm by corrosive combustion products. Of course, the inherent phase shift in the collected data due to the propagation delay through the probe tube has to be corrected afterwards. Since the probe tube is finite, small reflection effects remain in the transfer function of the probe microphone. The combustion chamber can be equipped with one microphone expandable up to three probe microphones at different axial positions. On the exhaust duct system sixteen microphones can be installed at four axial and four circumferential positions. From the acoustic time series, the downstream and upstream propagating acoustic waves can be determined using an in-house processing code for mode analysis. Thus, the total sound power emitted by the combustion system can be determined. The frequency range,

which is of importance for the investigations extends up to the cut-off frequency of the first higher mode. Therefore, only plane acoustic waves have to be taken into account. The first higher mode is an azimuthal wave at approximately 3.2 kHz, depending on the exhaust gas temperature. Temperature measurements with 0.001 inch thermocouples are possible at two positions. For both chamber materials a thermocouple is mounted in the throat of the outlet nozzle. In case of the steel combustion chambers an additional thermocouple can be installed inside. Steel and quartz glass were chosen as different cylinder materials to make additional pressure measurements in the combustion chamber via microphones possible or to have an optical access into the combustion chamber. Hence, measurements of OH-chemiluminescence were conducted for example to find a correlation between heat release fluctuation and sound radiation.

### 3. THEORETICAL ASPECTS

One of the first analytical considerations of sound generation by accelerated or decelerated entropy waves was published 1973 by Morfey (11). This work was an extension of the

Lighthill theory (9) for jet noise with the so called “excess jet noise” produced by density inhomogeneities in jets like for example in aero-engines. Following this analytical estimation by Morfey, the “excess jet noise” is scaling with the sixth power of the jet velocity. This extension of the Lighthill theory was further developed by Howe (7) who described the noise generation mechanisms in inhomogeneous and non-isentropic flows using an acoustic wave operator. In 1975 Ffowcs Williams & Howe (6) formulated an analytical expression for the sound generation and propagation of entropy inhomogeneities called slugs or pellets convecting through a nozzle. Using the Green function this formulation of Ffowcs Williams & Howe described the in-duct as well as the free field radiation of entropy induced sound in the time domain but it was restricted to low Mach number flows. The generation mechanism of entropy noise in one dimensional nozzle flows is characterized by Marble & Candel (10) for compact nozzles with subsonic and supersonic flow and supersonic flow with normal shocks. Here the compactness of the nozzle stands for a very small length of the nozzle compared to the wavelengths of the corresponding entropy and sound pressure waves. Marble & Candel derived expressions for the up- and downstream propagating acoustic pressure perturbations generated by both impinging entropy disturbances and impinging acoustic pressure waves. Therefore, these expressions result in the following three quasi transfer functions for either nozzle or diffuser configurations with subcritical mean flow conditions (see also (14)):

- For a sound pressure wave caused by entropy fluctuations:

$$p'_{2+} = \frac{M_2 - M_1}{1 + M_2} \frac{\frac{1}{2} M_1}{1 + \frac{1}{2} (\kappa - 1) M_1 M_2} a_1^2 A q'_s \quad (1)$$

- For the transmission of an entropy wave:

$$q'_{s2} = \left( \frac{1 + \frac{\kappa - 1}{\kappa} M_1^2}{1 + \frac{\kappa - 1}{\kappa} M_2^2} \right)^{\frac{1}{\kappa - 1}} q'_s \quad (2)$$

- For the transmission of an acoustic pressure wave:

$$T := \frac{p'_{2+}}{p'_{1+}} = \frac{1 + M_1}{M_1 + M_2} \frac{2M_2}{1 + M_2} \frac{1 + \frac{1}{2} (\kappa - 1) M_2^2}{1 + \frac{1}{2} (\kappa - 1) M_1 M_2} A \quad (3)$$

- with

$$A = \left( \frac{1 + \frac{1}{2} (\kappa - 1) M_1^2}{1 + \frac{1}{2} (\kappa - 1) M_2^2} \right)^{\frac{\kappa}{\kappa - 1}} \quad (4)$$

where  $\kappa$  is the isentropic exponent,  $M_1$  and  $M_2$  the Mach numbers upstream and downstream of the nozzle or diffuser, respectively,  $p'_{1+}$  the impinging acoustic pressure wave,  $q'_s$  the impinging density fluctuation corresponding to the entropy wave,  $q'_{s2}$  the transmitted density fluctuation through the nozzle or diffuser,  $a_1$  the speed of sound upstream of the nozzle or diffuser and  $p'_{2+}$  the downstream propagating acoustic pressure wave. The results of this one dimensional approach are compared with experimental data of this work in the result section.

## 4. MEASUREMENTS AND RESULTS

### 4.1. THE ENTROPY WAVE GENERATOR

The objective of the first series of measurements was the identification and separation of entropy noise from noise related to other sources. One of the fundamental characteristics of entropy noise is the slow propagation of the entropy waves or hot spots with the flow velocity compared to acoustic waves, which propagate with the speed of sound. The velocity of the tube flow in the test rig is about two orders of magnitude lower than the speed of sound. The second part of the measurements is a parametric study in order to evaluate the dependencies of entropy noise on the nozzle Mach number and on the amplitude of the temperature or entropy perturbation. Finally, these results are compared with the theoretically predicted values according to the one-dimensional theory of Marble & Candel (10).

#### 4.1.1. Entropy noise identification

In order to identify the generated entropy noise two different excitation modes have been used at the EWG:

1. In the pulse excitation mode, controlled by square pulses from a function generator, the platinum wires were heated once per second

with a pulse width of 10 or 100 ms. The received microphone signals were analysed in the time domain. An ensemble average over 300 single pulse traces was evaluated for each parameter variation.

2. Periodically heating of the EWG allowed cross-spectral analysis of the microphone signals and the excitation signal of the heating module.

In the time domain analysis of the pulse excitation mode, a distinct propagation delay between excitation signal and generated acoustic pressure downstream of the nozzle occurs. This time delay is mainly the result of the distance between heating module and nozzle divided by the tube flow velocity upstream of the nozzle. In the first part of the parametric study this distance has been varied in order to generate different propagation delays of the entropy waves.

Figure 3 shows the acoustic pressure pulse signals measured for three different tube lengths between heating module and nozzle. The bulk velocity in this tube section was 11.9 m/s and in the nozzle throat the Mach number amounted to  $Ma = 1$ . The heating current signal is plotted additionally in the graph as a dashed line. A positive temperature perturbation, induced by the heated

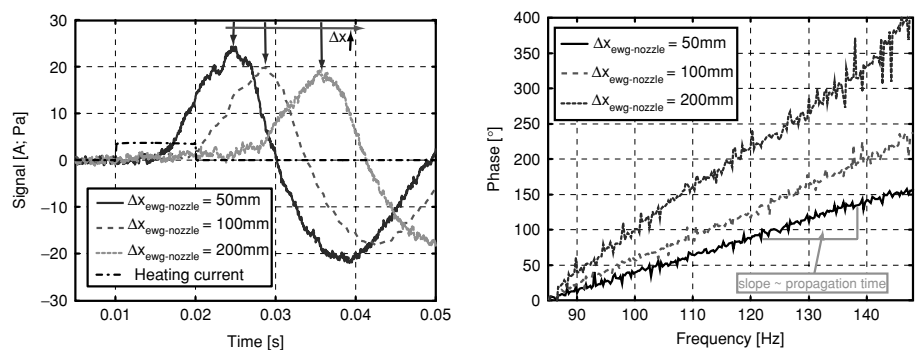


Figure 3. Phase averaged time series of the EWG microphone signals in the pulse excitation mode for different tube lengths  $\Delta x$  between heating module (EWG) and nozzle (left) and phase relation of cross spectra between heating current and microphone signals downstream of the nozzle for different tube between heating module (EWG) and nozzle (right).

platinum-wire module, generates a positive pressure pulse during its acceleration through the nozzle. The downstream propagating pressure pulse is detected by the wall-flush mounted microphones in the tube section behind the nozzle. The propagation delay of the entropy noise pressure pulse corresponds to the propagation path length between heating module and nozzle throat. An increasing tube length results in an increasing time delay of the pressure pulse. The slight decrease in the amplitudes of the pressure pulses with increasing duct length is caused probably by the increased dispersion of the entropy waves. The propagation or convection time of the entropy waves can also be determined in the periodical (sinusoidal) forced mode by cross-spectral analysis of microphone signals and excitation signals. The slope of the linear phase relation in the cross spectrum is anti-proportional to the propagation speed of the entropy wave.

The phase plot of the cross spectra between heating current and microphone signals downstream of the nozzle for an excitation sweep from about 85 Hz to 145 Hz is shown in Figure 3 (right). The different traces correspond to different tube lengths between heating module and nozzle throat. Due to the same propagation velocity the steepest phase line occurs for the longest distance ( $\Delta x_{EWG-nozzle} = 200$  mm). The phase relation has been used to quantify the propagation velocity, as shown in Tab. 1.

For the different tube lengths (column one) the time delay resulting

from the slope of the phase relation at different tube lengths is displayed in column two. Considering the acoustic propagation time of the generated entropy noise, the traveling speed of the entropy waves can be determined (column three). These phase velocities show a good agreement with the bulk velocity in the fourth column if it is taken into consideration that the bulk velocity is only a spatial mean value of the velocity profile in the tube calculated from the mass flux, the mean density and the tube cross-sectional area.

#### 4.1.2. Study on parameters of entropy noise

In order to evaluate the different parameters of entropy noise generation, a test series was carried out varying the amplitude of the temperature perturbation and the mass flux and therewith the nozzle Mach number. For the determination of the generated entropy noise the acoustic pressure pulse amplitude was extracted of a microphone signal measured downstream of the nozzle. The nozzle Mach number was changed from 0.15 up to 1.0 and amplitudes of temperature fluctuations between 1 K and 13 K were generated and measured by the bare thermocouple installed downstream of the heating module.

The generated entropy pressure pulse in the pulse excitation mode over the nozzle Mach number and the temperature fluctuation amplitude is displayed as contour plot in Figure 4. The entropy sound pressure increases

*Table 1. Propagation velocities of entropy waves calculated from phase relation in comparison with bulk velocity of the flow for different tube lengths  $Dx$  between heating module (EWG) and nozzle.*

Distance $\Delta x_{ewg-nozzle}$ [mm]	Time Delay [ms]	Propagation Velocity [m/s]	Bulk Velocity [m/s]
50	6.9	11.7	11.9
100	9.9	13.6	11.9
200	18.1	12.8	11.8

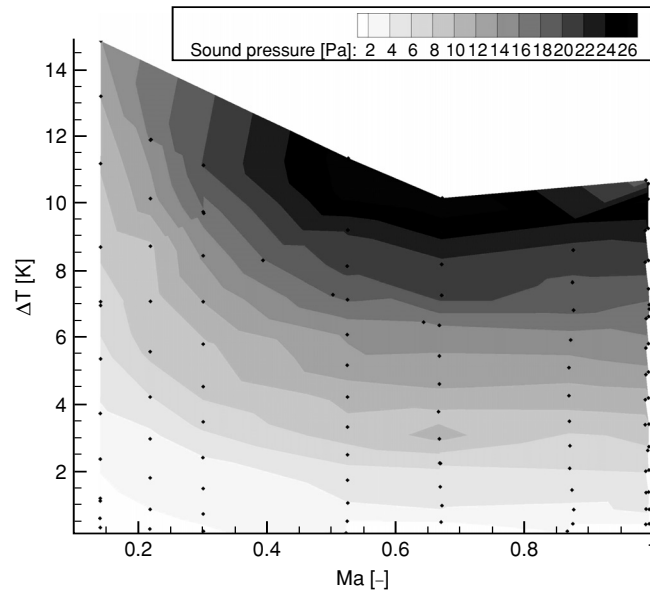


Figure 4. Acoustic pressure pulse amplitude of generated entropy noise at different nozzle Mach numbers and accelerated temperature or entropy perturbations.

with the accelerated temperature perturbation as well as the nozzle Mach number. However, Fig. 5 gives a deeper insight into the functional characteristics of temperature and Mach number as parameters for entropy noise.

Figure 5 (left) shows an almost linear relation between the temperature perturbation amplitude and the generated entropy noise amplitude for two different nozzle Mach numbers of  $Ma = 0.15$  and  $Ma = 1$ .

In contrast to the temperature, the dependency of entropy noise on the Mach number is not linear, as to be seen in Fig. 5 (right). For low nozzle Mach

numbers up to 0.7, the entropy sound pressure amplitudes are increasing with the Mach number as shown for two different temperature perturbation amplitudes of 7.5 K and 9 K. A decrease of the entropy sound pressure amplitude occurs for nozzle Mach number above 0.7. An explanation of this behavior could be the low acoustic transmission coefficient of the divergent part of the nozzle as predicted by Marble & Candel (10) for the acoustical characteristics of a diffuser flow at high inlet Mach numbers.

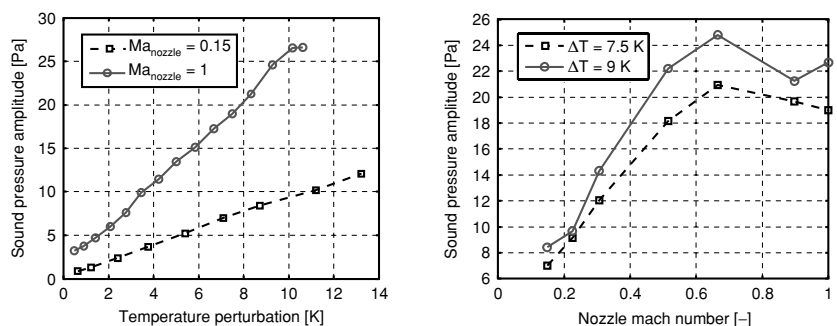


Figure 5. Acoustic pressure pulse amplitude of generated entropy noise over accelerated temperature perturbation for two different nozzle Mach numbers  $M_{anozzle} = 0.15$  and  $M_{anozzle} = 1$  (left) and acoustic pressure pulse amplitude of generated entropy noise over nozzle Mach number for two different amplitudes of accelerated temperature perturbation (right).

### 4.1.3. Comparison with theoretical prediction

The generation of entropy noise is described, in principle, for either a nozzle or a diffuser separately in the one dimensional theory of Marble & Candel (10). Since in the EWG a convergent-divergent nozzle was used, a combination of the theoretical expressions concerning the nozzle and the diffuser part of the set-up is necessary. The downstream propagating entropy pressure amplitude generated in the convergent nozzle has to be multiplied by the transmission factor of the subsequent diffuser. Furthermore, the pressure wave generated by the deceleration of the entropy wave in the diffuser has to be summed up to the total downstream propagating sound pressure wave for the comparison with the experimental data measured by the microphones in the duct section downstream of the nozzle.

The comparison of the experimental microphone data with the theory of Marble & Candel (10) is shown in Figure 6 displaying the entropy sound pressure amplitude normalized by the total pressure and divided by the normalized relative temperature perturbation over the nozzle Mach number. The different temperature amplitudes investigated in the parametric study for each nozzle

Mach number result in several marker points for a certain Mach number. The theoretical results are lower than the acquired data in case of low Mach numbers whereas for higher nozzle Mach numbers between 0.5 and 0.7 the experimental data and the predicted values show a good agreement. For the choked nozzle ( $Ma = 1$ ), the measured entropy noise amplitudes are lower than the theoretically predicted ones. The differences are not fully understood yet but a possible explanation could be the one-dimensional concept of the theory and the assumed compactness of the nozzle. The theory implies that the nozzle length has to be much smaller than the wavelengths of the entropy and the sound waves. This assumption may not be valid anymore, especially in case of the entropy wave which has a very short wavelength due to its low propagation speed. Furthermore, any radial velocity components and therewith correlated acceleration or deceleration occurring in the experimental nozzle flow are not included in the one-dimensional theory. The dashed lines in Figure 6 show power-law approximations for the theoretical data and the first inclining part of the experimental results. It is interesting to notice that the increase of the experimental entropy noise up to a nozzle Mach number of  $Ma = 0.5$  is proportional to  $Ma^{0.74}$  while the

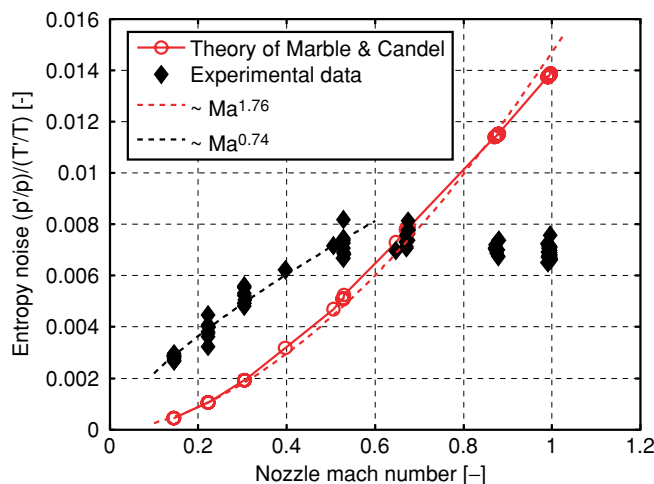


Figure 6. Comparison of experimental data with theoretical prediction; Normalized entropy sound pressure over nozzle Mach number.

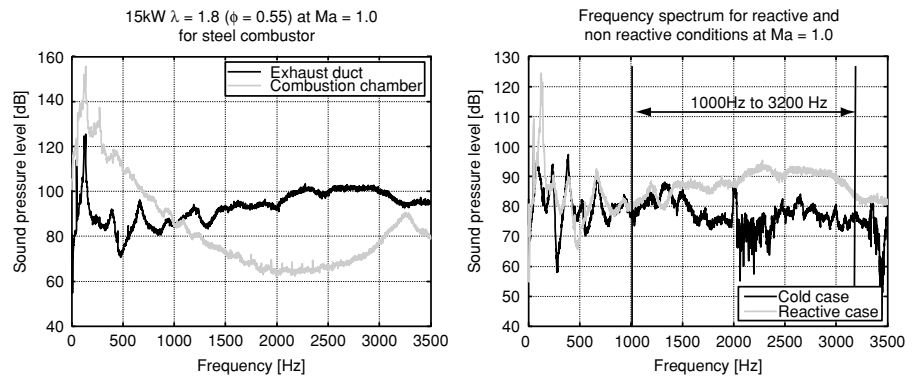


Figure 7. Comparison of sound pressure levels in combustion chamber and exhaust duct at  $\lambda = 1.8$  ( $\phi = 0.55$ ) and 15 kW (left) and sound pressure levels in the exhaust duct at same Mach number outlet condition ( $Ma = 1$ ) for reactive and nonreactive conditions.

corresponding theoretical data is proportional to a power law of  $Ma^{1.76}$ .

#### 4.2. COMBUSTOR

During the experiments on the model combustor test rig differences in sound pressure levels between combustion chamber and exhaust duct especially at high Mach number outlet conditions can be observed. Figure 7 (left) compares the sound pressure levels of two microphones mounted in the combustion chamber and the exhaust duct at 15 kW power consumption and an equivalence ratio of  $\phi = 0.55$ . It can be seen that waves of the dominating frequencies propagate from combustion chamber to exhaust duct via the chamber outlet nozzle. Especially in the high frequency region (higher than 1 kHz) an increased sound pressure level in the exhaust duct is remarkable - differences up to 30dB can be recognized. The combustion chamber is much noisier than the exhaust duct in the low frequency region because lower frequencies are dominated by combustion noise. Since only the outlet nozzle is installed between combustion chamber and exhaust pipe an additional noise generating mechanism can be assumed inside this nozzle producing sound in the higher frequency region. To exclude turbulent flow noise as a possible origin for this additional noise

the acoustic field of a comparable cold flow was contrasted to the reactive case (see Fig. 7 (right)). For this kind of nozzle flows the throat Mach number is a significant parameter for turbulent flow noise and allows the comparison of hot and cold flow conditions. Nonreactive/cold conditions are established by an air flow through the combustion chamber without methane and therefore without combustion. For identical microphone positions in the exhaust duct and same nozzle Mach numbers but different conditions in the combustion chamber broadband noise is lower in amplitude for cold conditions (see Fig. 7 (right)). If turbulent flow noise would be the only noise source both curves should look similar.

In order to achieve a better quantification of this broadband noise phenomenon the SPLs were summed up for frequencies from 1 kHz to 3.2 kHz and plotted to show the dependency on the nozzle throat Mach number. This more general overview for a steel combustor with normal length is provided by Fig. 8. In both images the summed up sound pressure levels in the combustion chamber and in the exhaust duct for cold respectively reactive conditions are determined and plotted versus the Mach number at minimum cross-sectional area in the exhaust nozzle. Different curves in the reactive

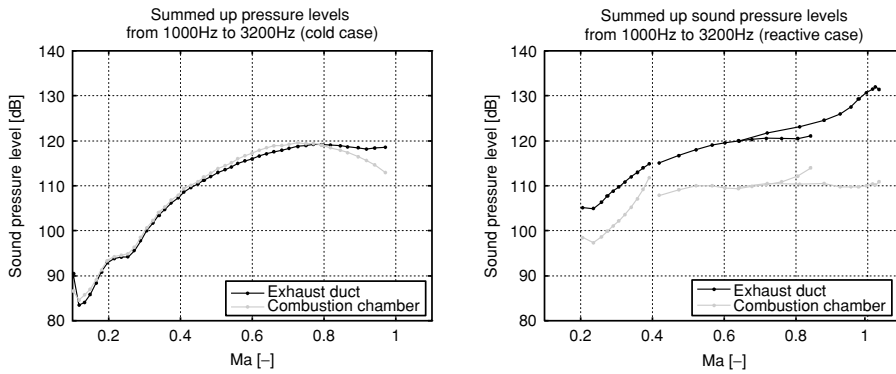


Figure 8. Summed up sound pressure levels in combustion chamber and exhaust duct versus Mach number for cold flow (left) and reactive flow (right) conditions.

case result from different power consumption, e.g. the first region of  $Ma = 0.1$  to nearly  $0.4$  relates to the  $5\text{ kW}$  case followed by the  $10\text{ kW}$  case for  $Ma = 0.45$  to  $0.85$ . Overlapping Mach numbers can be observed in the region of  $Ma = 0.6$  to  $0.85$ . Here the  $10\text{ kW}$  power consumption for lean combustion produces similar outlet conditions in the nozzle compared to the rich combustion at  $15\text{ kW}$  power consumption. For nonreactive conditions the summed up SPLs from  $1\text{ kHz}$  to  $3.2\text{ kHz}$  are quite similar except for a small region near  $Ma = 1$ . For reactive conditions the summed up SPLs in the exhaust duct are always higher than the SPLs in the combustion chamber and the discrepancy increases with higher Mach numbers. That indicates an additional noise source for the reactive case compared to the cold case. Since only the exhaust nozzle is installed between the combustion chamber and the exhaust duct the noise generation mechanism must be located inside the nozzle and must depend on the Mach number.

The results of summed up sound pressure levels may be distorted by reflections or interference noise caused by the flow. Furthermore it cannot be ignored that partly noise emissions may be generated by turbulent flow noise through the nozzle. That may explain the small differences in the summed up sound pressure levels between exhaust

duct and combustion chamber for cold flow conditions. Therefore, Figure 9 (left) shows the dependency of the emitted sound power in the exhaust duct investigating different combustor materials and lengths at different Mach numbers. The sound power can be derived by decomposition the sound field into forward and backward traveling waves. Considering only forward traveling plane waves the emitted sound power can be calculated. That eliminates the influence of reflecting waves. To overcome the interference noise caused by the flow the three microphone method (4) was applied during decomposition. A similar increase of the sound power compared to the SPLs can be calculated. It seems that neither different combustor wall temperatures, provided by different materials (steel/glass), nor different mixing conditions for temperature inhomogeneities (double combustion chamber length allows a better mixing than the normal length) change the acoustic output power of the combustion system in this frequency range. Different materials should have different thermal radiation. That definitely changes the combustion process and the peak frequency of the system but did not influence the sound emission in higher frequency regions. In addition to the decomposition a calculation of the reflection coefficient in the exhaust duct is possible, that

provides low pressure reflection coefficients in the range over 1 kHz. It can be shown that in this region the coefficient is below 50 percent. That qualifies the comparison of SPLs for frequencies higher than 1 kHz as shown in Fig. 7 and 8, therein discrepancies between exhaust duct and combustion chamber are obvious for all operating conditions. The ratio between the sound pressure levels in exhaust duct and combustion chamber for reactive conditions shows a significant higher increase in sound pressure in the exhaust duct at higher Mach numbers, up to a ratio of 12 (see Fig 9 (right)). Entropy noise may explain the differences between cold and reactive conditions caused by the acceleration of temperature inhomogeneities. An increase in sound emission with increasing Mach number can be derived from the theory which is particularly applicable to reactive conditions where entropy fluctuations are significant. Since no temperature fluctuations exist for cold conditions the slope is comparatively gentle. The gap between the overlapping Mach numbers from  $Ma = 0.6$  to  $0.85$  at reactive conditions may be explained by minor temperature fluctuations at lower power consumptions leading to a lower sound emission. However, an increase in the emitted sound power with increasing Mach number is detectable for all

different combustion chambers corresponding to the theory of entropy noise.

## 5. CONCLUSION

Entropy noise was investigated in two different test facilities in which entropy waves were either generated by electrical heating or by the combustion of methane. A parameter study on the entropy noise generation mechanism performed at the EWG showed the expected linear dependence of the induced entropy sound pressure amplitude on the amplitude of the entropy or temperature perturbation. The correlation of the entropy noise with the nozzle Mach number indicated a strongly increasing entropy noise pressure with the Mach number in case of low Mach numbers, whereas for Mach numbers higher than  $0.8$ , the entropy noise is slightly decreasing. The experimental data was compared to the theory of Marble & Candel (10). Taking into account the simplifying assumptions, such as a one-dimensional description, the theory gives a reasonable estimate of noise level around a Mach number of  $0.6$ ; it shows a broadly similar trend below  $M_{\text{anozzle}} = 0.6$ ; for  $M_{\text{anozzle}} > 0.6$  there is a saturation effect in the experimental noise levels which is absent in the theory.

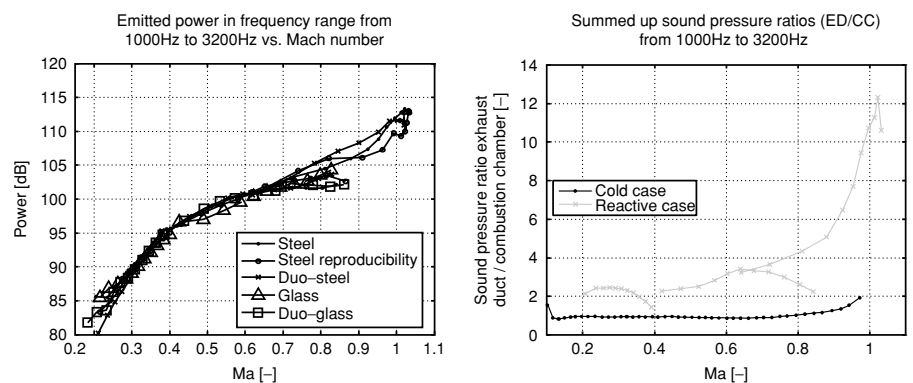


Figure 9: Emitted sound power (1-3.2 kHz) in the exhaust duct (left) and ratio of summed up exhaust duct/combustion chamber sound pressure levels versus Mach number for nonreactive and reactive conditions (right).

In the exhaust pipe of the gas turbine model combustor the occurrence of broadband sound emission in the region of 1 kHz to 3 kHz independent of changes in geometry or material was found. That phenomenon, probably related to entropy noise, has also been observed in aero-engines in the interaction between combustion chamber and high pressure turbine and is called “core noise”. This “core noise” has a strong relevance especially for turboshaft engines since there occurs hardly any jet noise on the exhaust side of the engine.

## 6. ACKNOWLEDGEMENT

The authors gratefully acknowledge the financial support by the German Research Foundation (DFG) through the research unit FOR 486 “Combustion Noise”. We also would like to thank Prof. Dr. Ulf Michel for the profitable discussions. Thanks go to Prof. Dr. Oliver Paschereit (TU Berlin) for his contribution to this work.

## REFERENCES

- [1] Bake F. and Michel U. and Röhle I., 2007 “Investigation of Entropy Noise in Aero-Engine Combustors”. *J. of Engineering for Gas Turbines and Power* 129(2), April, pp.370–376.
- [2] Bohn, M. S., 1976. “Noise produced by the interaction of acoustic waves and entropy waves with high-speed nozzle flows”. PhD thesis, California Institute of Technology, Pasadena, California, USA, April.
- [3] Cumpsty N.A., 1979, “Jet engine combustion noise: pressure, entropy and vorticity perturbations produced by unsteady combustion or heat addition”. *J. Sound Vibration*, 66(4), pp. 527–544.
- [4] Chung J.Y., 1977, “Rejection of flow noise using coherence function method”. *Journal of the Acoustical Society of America*, 62, pp. 388–395.
- [5] Dowling, A. P., 1996. “Acoustics of unstable flows”. In *Theoretical and Applied Mechanics*, T. Tatsumi, E. Watanabe, and T. Kambe, eds., Elsevier, Amsterdam, pp. 171–186.
- [6] Ffowcs Williams, J. E., and Howe, M. S., 1975. “The generation of sound by density inhomogeneities in low Mach number nozzle flows”. *J. Fluid Mech.*, 70, November, pp. 605–622. part 3.
- [7] Howe, M. S., 1975. “Contributions to the theory of aerodynamic sound, with application to excess jet noise and the theory of the flute”. *J. Fluid Mech.*, 71, pp. 625–673. part 4.
- [8] Kovaszny, L. S. G., 1953. “Turbulence in supersonic flow”. *Journal of the Aeronautical Sciences*, 20(10), October, pp. 657–682.
- [9] Lighthill, M. J., 1952. “On sound generated aerodynamically”. *Proc. R. Soc. Lond. A*(211), pp. 564–587.
- [10] Marble, F. E., and Candel, S. M., 1977. “Acoustic disturbances from gas non-uniformities convected through a nozzle”. *J. Sound Vibration*, 55(2), pp. 225–243.
- [11] Morfey, C. L., 1973. “Amplification of aerodynamic noise by convected flow inhomogeneities”. *J. Sound Vibration*, 31(4), pp. 391–397.
- [12] Mühlbauer, B., Widenhorn, A., Liu, M., Noll, B., and Aigner, M., 2007. “Fundamental mechanism of entropy noise in aero-engines: Numerical simulation”. In *ASME Turbo Expo 2007*, no. GT2007-27173, ASME.
- [13] Muthukrishnan, M., Strahle, W. C., and Neale, D. H., 1978. “Separation of Hydrodynamic, Entropy, and Combustion Noise in a Gas Turbine Combustor”. *AIAA Journal*, 16(4), pp. 320–327.
- [14] Schemel, C., 2003. “Modellierung und numerische Simulation der Entstehung und Ausbreitung von Schall durch Entropiewellen in beschleunigten Rohrströmungen”. Diplomarbeit, Technische Universität Berlin, Berlin.
- [15] Schemel, C., Thiele, F., Bake, F. Lehmann, B. and Michel U., 2004. “Sound Generation in the Outlet Section of Gas Turbine Combustion Chambers”. 10th AIAA/CEAS Aeroacoustics Conference, Manchester, UK, May, 2004-2929.
- [16] Strahle, W. C., 1971 “On combustion generated noise” *J. Fluid Mech.*, 49(2), pp.399–414.
- [17] Strahle, W. C., and Muthukrishnan, M., 1976. “Thermocouple time constant measurement by cross power spectra”. *AIAA Journal*, 14(11), November, pp. 1642–1644.
- [18] Strahle, W. C., Muthukrishnan, M., and Neale, D. H., 1977. “Experimental and analytical separation of hydrodynamic, entropy and direct combustion noise in a gas turbine combustor”. In *AIAA 4th Aeroacoustic Conference*, no. 77-1275, AIAA.
- [19] Strahle, W. C., 1978. “Combustion noise”. *Prog. Energy Combust. Sci.*, 4(3), pp. 157–176. A.
- [20] Zukoski, E. E., and Auerbach, J. M., 1976. “Experiments concerning the response of supersonic nozzles to fluctuating inlet conditions”. *Journal of Engineering for Power* (75-GT-40), January, pp. 60–63. ASME.

#### **LIBERTYVILLE STOPS WIND TURBINE**

A wind turbine that recently was installed at a Libertyville (IL) business has been deactivated because of neighbours' complaints about noise. The 120ft tall, three bladed windmill was shut down after Lake County Judge Mitchell Hoffmann signed a temporary restraining order.

#### **NOISY INDUSTRY TRIES TO STOP HOUSING BEING BUILT NEARBY**

Plans to build hundreds of homes at a former Northumberland pit look set to be approved – despite fears that families living in them could suffer noise nuisance from a nearby port terminal. Mining and development company the Banks Group wants to build 327 houses and apartments on the disused site of Bates Colliery in Blyth, which closed more than 20 years ago. This week county councillors will be recommended to give their backing to the scheme, which planning officials say will assist with the housing-led regeneration of the River Blyth Estuary and get rid of a derelict and contaminated area of land. However, bosses at the Port of Blyth have lodged a formal objection, claiming future residents of the homes could suffer 'significant disturbance' from noise generated by operations at the nearby Bates bulk export terminal. The terminal loads cargoes such as coal, grain and glass onto ships, and port chiefs fear statutory noise complaints from people living in the new dwellings would risk restricting the port's future operations. Port chief executive Martin Lawlor says the export operation is 'inherently noisy', and in some cases also dusty. "Bates Terminal is ideally suited for development for a range of other port-related uses such as container handling, scrap loading and metal handling. All of these uses would be significantly noisier." Were housing constructed, it is not impossible, even if new residents were warned of noise beforehand, that they could bring an action against the Port, or organisations which operate in the Port.